Switching the Mechanism of Spin-Exchange Coupling in a (μ-Oxo)bis(μ-acetato)chromium(III)vanadium(III) Complex by Protonation of the Oxo Bridge

Rainer Hotzelmann and Karl Wieghardt*

Lehrstuhl für Anorganische Chemie I, Ruhr-Universität, D-4630 Bochum, Germany

Received May 4, 1992

Introduction

Recently we have shown that strong spin-exchange coupling occurs in the oxo-bridged homodinuclear complexes I[1] and II[2] (Scheme I), both of which contain a (μ-oxo)bis(μ-acetato)dimetal(III) core. Fairly weak antiferromagnetic coupling has been observed in I ($H = -2JS_1 \cdot S_2$; $S_1 = S_2 = {}^3/_2$; $J = -32$ cm^{-1}; $S =$ 0 ground state) whereas for II strong ferromagnetic coupling has been reported ($S_1 = S_2 = 1$; $J > +200$ cm^{-1}; $S = 2$ ground state). Interestingly, in the asymmetric heterodinuclear chromium(III)-vanadium(III) species III, the spins are also ferromagnetically coupled[3] ($S_1 = {}^3/_2$; $S_2 = 1$; $J > 100$ cm^{-1}; $S = {}^5/_2$ ground state). Both I and II may be reversibly protonated at the oxo bridge with formation of homodinuclear μ-hydroxo complexes Ia[4] and IIa.[2a] The nature of the spin-exchange coupling does not change upon protonation of I; but a significantly smaller antiferromagnetic coupling is observed in Ia ($J = -15$ cm^{-1}). In contrast, protonation of II resulted in a switching of the mechanism of the spin-exchange coupling from ferromagnetic in II to antiferromagnetic in IIa.[2a] We decided that it would be of interest to study the effect of protonation of III on the magnetic properties of the resulting μ-hydroxo species IIIa.

Experimental Section

The ligands 1,4,7-triazacyclononane ($C_6H_{15}N_3$; L) and 1,4,7-trimethyl-1,4,7-triazacyclononane ($C_9H_{21}N_3$; L')[5] and the complex [L'Cr(μ-O)(μ-$CH_3CO_2)_2$VL]$(ClO_4)_2$[3] have been prepared as described previously.

Synthesis of [L'Cr(μ-OH)(μ-$CH_3CO_2)_2$VL]$(ClO_4)_3$ (IIIa). To a green deoxygenated methanolic solution (20 mL) of [L'Cr(μ-O)(μ-$CH_3CO_2)_2$-VL]$(ClO_4)_2$ (0.15 g; 0.20 mmol) were added a few drops of concentrated $HClO_4$ at room temperature. A color change to pink occurred, and a pink microcrystalline material precipitated immediately, which was collected by filtration, washed with diethyl ether, and air-dried. Yield: 0.15 g (90%). IR (KBr disk): ν_{as}(C–O) 1586, ν_s(C–O) 1461 cm^{-1}. UV–vis (CH_3CN): 320 nm (sh, $\epsilon \approx 840$ M^{-1} cm^{-1}), 375 (sh, 190), 400 (sh, 160), 415 (sh, 120), 521 (150), 660 (sh, 7), 688 (6), 705 (4). Anal. Calcd for [$C_{19}H_{43}CrN_6O_5V$]$(ClO_4)_3$: C, 27.3; H, 5.2; N, 10.0; Cr, 6.2; V, 6.1. Found: C, 26.9; H, 5.3; N, 9.8; Cr, 6.0; V, 5.9.

Physical Measurements. The equipment used for recording electronic spectra and cyclic voltammograms has been described previously.[2a] X-Band EPR spectra of solid samples of III and IIIa were recorded on a Bruker ER 200 DX-band spectrometer equipped with a standard Te202 resonator (ER 4102, Bruker) and a helium flow cryostat. Measurements of the magnetic susceptibility of complexes were performed on powdered samples in the temperature range 3–295 K on a SQUID magnetometer (MPMS, Quantum Design). Data were evaluated by using the standard software of the instrument and corrected for the diamagnetic response of the holder and diamagnetism of the sample by using Pascal's constants.

Scheme I.

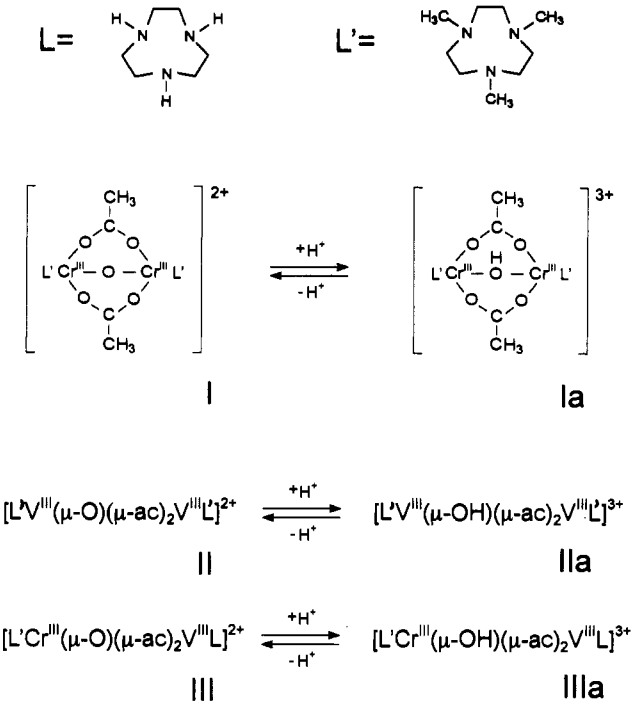

Results

Acidification with $HClO_4$ of a dark green methanolic solution of [L'Cr^{III}(μ-O)(μ-$CH_3CO_2)_2V^{III}$L]$(ClO_4)_2$ (III) effects an immediate color change to pink and initiates the precipitation of [L'Cr^{III}(μ-OH)(μ-$CH_3CO_2)_2V^{III}$L]$(ClO_4)_3$ (IIIa). The protonation is reversible, as is readily demonstrated by the re-formation of the dark green solution by addition of triethylamine. The drastic change of the UV–visible spectrum of III upon protonation to yield IIIa is shown in Figure 1. Aqueous solutions of III and IIIa—even under anaerobic conditions—are only moderately stable at room temperature.

The dissociation constant for reaction 1 has been determined spectrophotometrically at 378 nm by using a range of aqueous

$$\text{IIIa} \rightleftharpoons \text{III} + H^+ \quad K_a \qquad (1)$$

buffer solutions (pH 3–10). A pK_a value of ≈7.5 has been determined at 20 °C. The corresponding value for the homodinuclear species II and IIa is 0.9,[2a] and for I and Ia the pK_a value is estimated to be between 8 and 9.

Figure 2 shows the cyclic voltammograms of III and IIIa in CH_3CN (0.10 M tetra-*n*-butylammonium hexafluorophosphate supporting electrolyte; glassy carbon working electrode; Ag/AgCl (saturated LiCl/C_2H_5OH) reference electrode) in the potential range +1.20 to −1.40 V vs Ag/AgCl. III is reversibly oxidized by one electron at $E^1_{1/2} = +0.01$ V vs NHE, whereas IIIa is

$$[Cr^{III}\text{–O–}V^{III}]^{2+} \underset{+e^-}{\overset{-e^-}{\rightleftharpoons}} [Cr^{III}\text{–O–}V^{IV}]^{3+} \quad E^1_{1/2} \qquad (2)$$

$$[Cr^{III}\text{–OH–}V^{III}]^{3+} \underset{-e^-}{\overset{+3^-}{\rightleftharpoons}} [Cr^{III}\text{–OH–}V^{II}]^{2+} \quad E^2_{1/2} \qquad (3)$$

reversibly reduced at $E^2_{1/2} = -0.65$ V vs NHE by one electron, as has been established by controlled-potential coulometry. The CV of IIIa also shows a small reversible wave at $E_{1/2} = 0.01$ V

(1) Martin, L. L.; Wieghardt, K.; Blondin, G.; Girerd, J.-J.; Nuber, B.; Weiss, J. *J. Chem. Soc., Chem. Commun.* **1990**, 1767.
(2) (a) Knopp, P.; Wieghardt, K. *Inorg. Chem.* **1991**, *30*, 4061. (b) Köppen, M.; Fresen, G.; Wieghardt, K.; Llusar, R. M.; Nuber, B.; Weiss, J. *Inorg. Chem.* **1988**, *27*, 721. (c) Knopp, P.; Wieghardt, K.; Nuber, B.; Weiss, J.; Sheldrick, W. S. *Inorg. Chem.* **1990**, *29*, 363.
(3) Hotzelmann, R.; Wieghardt, K.; Flörke, U.; Haupt, H.-J.; Weatherburn, D. C.; Bonvoisin, J.; Blondin, G.; Girerd, J.-J. *J. Am. Chem. Soc.* **1992**, *114*, 1681.
(4) (a) Chaudhuri, P.; Winter, M.; Küppers, H.-J.; Wieghardt, K.; Nuber, B.; Weiss, J. *Inorg. Chem.* **1987**, *26*, 3302. (b) Reber, C.; Güdel, H. U.; Buijs, M.; Wieghardt, K.; Chaudhuri, P. *Inorg. Chem.* **1988**, *27*, 2115.
(5) (a) Wieghardt, K.; Schmidt, W.; Nuber, B.; Weiss, J. *Chem. Ber.* **1979**, *112*, 2220. (b) Wieghardt, K.; Chaudhuri, P.; Nuber, B.; Weiss, J. *Inorg. Chem.* **1982**, *21*, 3086.

0020-1669/93/1332-0114$04.00/0

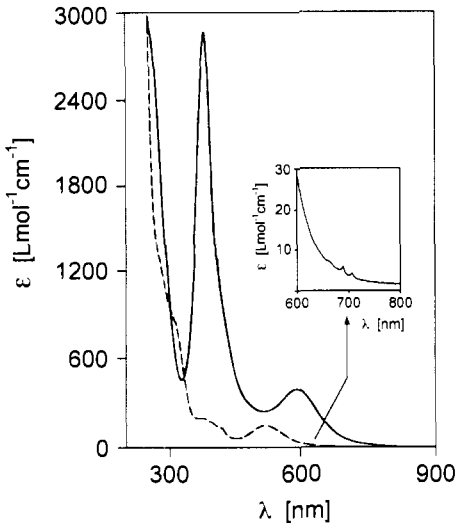

Figure 1. Electronic spectra of III (—) and IIIa (- - -) in acetonitrile at 20 °C. The inset shows the spectrum of IIIa in the region 600–800 nm.

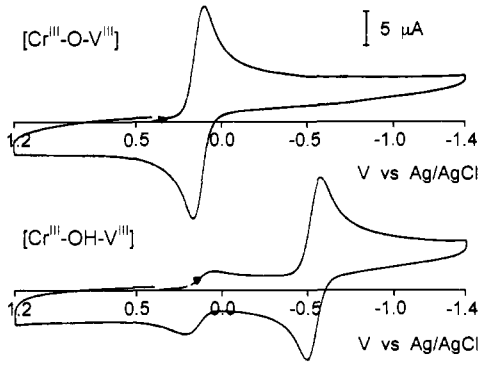

Figure 2. Cyclic voltammograms of III and IIIa in acetonitrile at 22 °C (0.10 M tetra-*n*-butylammonium hexafluorophosphate supporting electroltye; [complex] ~ 10^{-3} M; glassy carbon working electrode, Pt-wire auxiliary electrode, Ag/AgCl (saturated LiCl; C_2H_5OH) reference electrode; scan rate 200 mV s^{-1}).

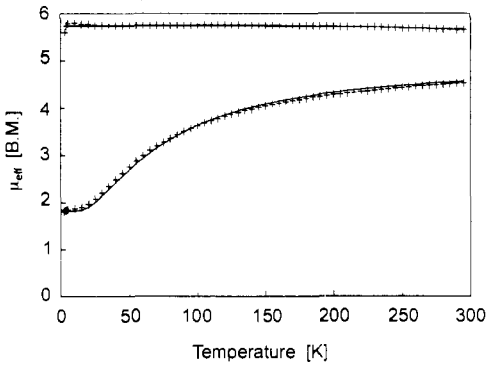

Figure 3. Temperature dependence of the magnetic moment μ_{eff}/μ_B of III (upper trace) and IIIa (lower trace): +, experimental data; solid line, least-squares best fit to the data (see text).

vs NHE, which is due to the presence of a small impurity of III. The redox potentials, the peak separation $E_{p,ox} - E_{p,red}$ of ≈70 mV, and the ratio $I_{p,a}/I_{p,c}$ of ≈1.0 were found to be independent of the scan rate (50–500 mV s^{-1}). Oxidation of III most probably involves metal-centered oxidation of the vanadium(III) ion to V(IV), and in IIIa it is probably again the vanadium(III) ion which is reduced to V(II). Both the oxidized form of III and the reduced form of IIIa have not been isolated.

Figure 3 shows the magnetic moments of III and IIIa in the temperature range 3–295 K. For III a temperature-*independent* magnetic moment of 5.7 μ_B was found, which clearly indicates an $S = {}^5/_2$ ground state originating from strong *ferromagnetic*

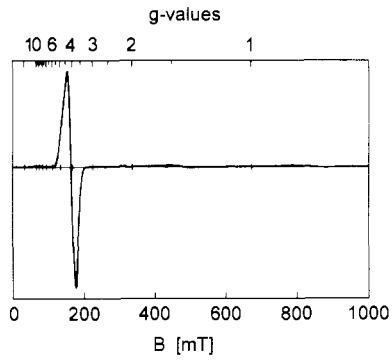

Figure 4. X-Band EPR spectrum of the solid tetraphenylborate salt of III at 40 K (microwave frequency 9.4363 GHz; dX''/dB = 20 μW/40 dB).

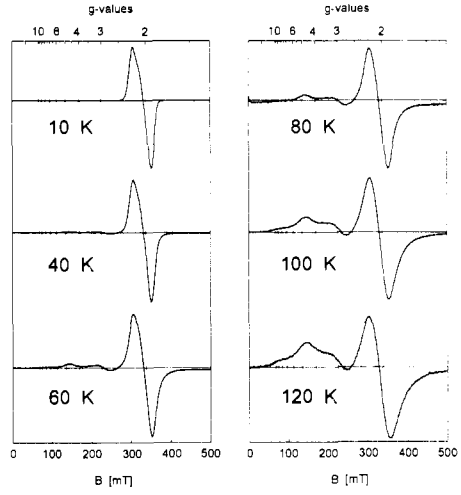

Figure 5. Temperature-dependent X-band EPR spectra of solid IIIa (9.4376 GHz (10 K); 9.4385 GHz (40–120 K); dX''/dB = 20 μW/40 dB (10–80 K); 200 μW/30 dB (100, 120 K)).

coupling of a Cr(III)(d^3) and a V(III)(d^2) ion. In contrast, the magnetic moment of IIIa is temperature-*dependent*; it decreases from 4.5 μ_B at 295 K to 1.9 μ_B at 15 K, where it reaches a plateau. From 10 to 2 K the magnetic moment of 1.84 μ_B is temperature-independent. This behavior is typical for intramolecular antiferromagnetic spin-exchange coupling between a chromium(III)(d^3) and a vanadium(III)(d^2) ion. IIIa has an $S = {}^1/_2$ ground state. The temperature dependence has been successfully modeled by using the usual isotropic Heisenberg–Dirac–Van Vleck model for spin exchange with the spin-Hamiltonian $H = -2JS_1 \cdot S_2$ where $S_1 = {}^3/_2$ and $S_2 = 1$.[6] A least-squares best fit to the data yielded the spin-exchange-coupling constant $J = -19$ cm^{-1}. Thus the nature of the spin coupling changes upon protonation of III at the μ-oxo group.

X-Band EPR spectra of powdered crystalline samples of III and IIIa have been recorded in the temperature range 2.7–200 K (Figures 4 and 5). The spectrum of III is temperature-independent. A typical rhombic signal of an $S = {}^5/_2$ spin system is observed. No vanadium hyperfine structure is observed. From resonances at $g_1 = 4.1$, $g_2 = 1.4$, and $g_3 = 9.5$, the rhombicity factor $\lambda = E/D$ is estimated to be ≈0.3. This spectrum nicely corroborates the susceptibility measurements of III. In contrast, the X-band EPR spectrum of solid IIIa is strongly temperature-dependent (Figure 5). In the temperature range 2.7–10 K a nearly isotropic signal at $g \approx 2.0$ is observed, in agreement with an $S = {}^1/_2$ ground state of IIIa. With increasing temperature new features at $g > 2.0$ appear. At 40 K two new weak signals are observed at $g = 3.0$ and 4.6, which correspond to $\mathbf{g}_x$ and $\mathbf{g}_y$ tensors of a rhombic excited $S = {}^3/_2$ state ($\lambda \approx 0.2$). At

(6) O'Connor, C. J. *Prog. Inorg. Chem.* **1982**, *29*, 1203.

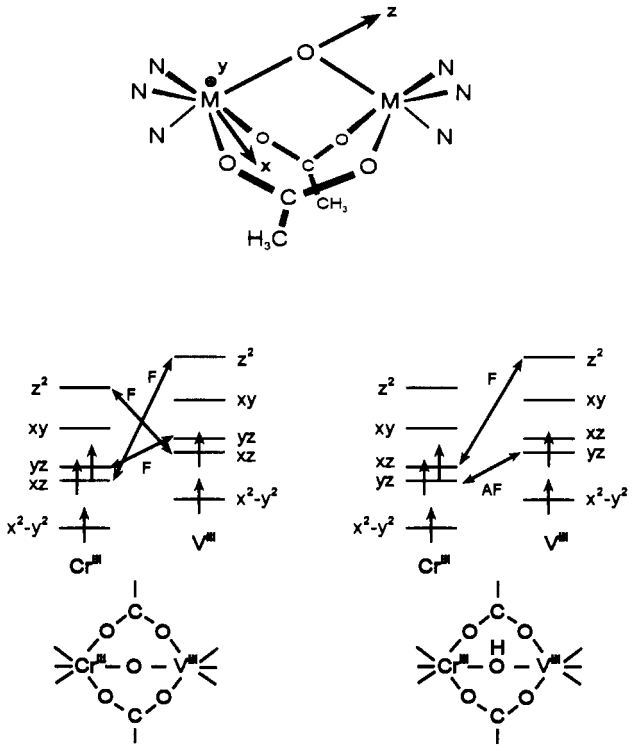

Figure 6. Schematic representation of the energetic order (orbitrary scale) of d orbitals and symmetry-allowed orbital interactions with p orbitals of the O^{2-} bridge (not shown) which lead to ferromagnetic (F) or antiferromagnetic (AF) spin-exchange coupling in III (left-hand side) and IIIa (right-hand side).

temperatures above 100 K a further signal at $g \approx 8$–9 is detected. The intensity of this and of all other signals increases with further increase of the temperature. The latter signal belongs to an excited $S = {}^5/_2$ state (g_y). Thus the EPR spectra of IIIa are fully in accord with the notion that the spins of the chromium(III) and vanadium(III) ions in IIIa are intramolecularly antiferromagnetically coupled, yielding an $S = {}^1/_2$ ground state and $S = {}^3/_2$, ${}^5/_2$ excited states.

Discussion

We have recently published an analysis of the relevant interacting magnetic orbitals for first-row transition metal complexes containing the (μ-oxo)bis(μ-carboxylato)dimetal core.[2a,3] The magnetism of III is readily understood in the framework of this model. For the following discussion we will use the coordinate system as is defined in Figure 6. Note that this choice of coordinates changes the conventional designation of d orbitals in an octahedral ligand field: $d_{xy} \rightarrow d_{x^2-y^2}$; $d_{x^2-y^2} \rightarrow d_{xy}$ (d_{z^2} and d_{xz}, d_{yz} remain unchanged). We have shown that only three symmetry-allowed orbital interactions are important in the given structure type: (i) the d_{z^2} atom orbitals of both metal ions interact with a filled p orbital of the oxo bridge ($d_{z^2}|p|d_{z^2}$);[7] (ii) two d_{yz} atom orbitals interact with a p orbital of the oxo group ($d_{yz}|p|d_{yz}$); and (iii) there is a strong overlap between a d_{xz} orbital at metal 1, a p orbital of the O^{2-} ion, and a d_{z^2} orbital at metal 2 ($d_{xz}|p|d_{z^2}$). For a pictorial representation see Figure 6 in ref 2a. Due to the fact that the M–O_{oxo} bond is the shortest metal–ligand bond in all $[L'M^1(\mu\text{-}O)(\mu\text{-}CH_3CO_2)_2M^2L]^{2+}$ complexes, the energetic order of orbitals is as qualitatively shown in Figure 6 (left-hand side). In the present $Cr^{III}V^{III}$ complexes the $d_{z^2}|p|d_{z^2}$ pathway does not contribute to the magnetism of III and IIIa since the d_{z^2} orbitals of both metal ions are empty.

According to the Goodenough–Kanamori rules for magnetic superexchange[7,8] the interaction ii leads to antiferromagnetic coupling if the d_{yz} orbitals at both metal ions are half-filled. If, on the other hand, the d_{yz} orbital at the metal 1 is half-filled and the other at metal 2 is empty, *ferromagnetic* coupling results. The same arguments hold for interaction iii. It is then obvious that both the ($d_{yz}|p|d_{yz}$) and the ($d_{xz}|p|d_{z^2}$) interactions lead to ferromagnetic superexchange in III; no antiferromagnetic pathway is available if the energetic ordering of orbitals is as in Figure 6 (left-hand side).

This model requires that the degeneracy of the d_{xz} and d_{yz} orbitals at both metal ions be lifted and that the d_{xz} orbitals at both metal ions be lower in energy than the d_{yz} orbitals. If this energetic order is reversed (Figure 6, right-hand side) the $d_{yz}|p|d_{yz}$ interaction now provides an antiferromagnetic pathway whereas the ($d_{xz}|p|d_{z^2}$) interaction still yields ferromagnetic coupling. Since the sign of the spin-exchange-coupling constant J results from the sum of ferro- and antiferromagnetic contributions (eq 4), it

$$J = J_{AF} + J_F \qquad (4)$$

follows that both weak anti- and ferromagnetic coupling may be anticipated. Antiferromagnetic coupling usually is stronger than ferromagnetic,[8] and therefore, weak antiferromagnetic coupling is expected to be dominant. This is the case of IIIa, where an $S = {}^1/_2$ ground state is observed.

Protonation of the oxo bridge results in a significant lengthening of the metal–oxygen bond distance, and consequently, the orbital overlap is reduced, which at the same time reduces the magnitude of ferro- and antiferromagnetic spin-exchange coupling; in addition, it may bring about the reversal of energetic ordering of the d_{xz} and d_{yz} metal orbitals.

Acknowledgment. We thank Dr. E. Bill and Dipl. Phys. C. Butzlaff (Medizinische Universität Lübeck, Germany) for recording the EPR spectra and the magnetic susceptibility data. Financial support of this work by the Fonds der Chemischen Industrie is also gratefully acknowledged.

(7) The designation of these orbital interactions is as in: Ginsberg, A. P. *Inorg. Chim. Acta Rev.* **1971**, *5*, 45.
(8) Goodenough, J. B. *Magnetism and the Chemical Bond*; Interscience Publishers: New York, 1963.